Regular Paper

Title:

Searching for Acrolein-Scavenging Compounds in Plants: Isoalliin from Onion as an Excellent Scavenger

Running head:

Acrolein scavenging compounds in plants

Authors:

Ayako Hada [a], Chihiro Nozaki [b], Natsumi Tamura [b], Kenji Matsui [a], Yasumasa Matsuoka [c], Daisuke Shibata [d#], Jun'ichi Mano [a,e,f*†]

Affiliations:

[a] Graduate School of Sciences and Technology for Innovation, Yamaguchi University, Yoshida 1677-1, Yamaguchi 753-8515, Japan

[b] Faculty of Agriculture, Yamaguchi University, Yoshida 1677-1, Yamaguchi 753-8515, Japan

[c] Advanced Technology Institute, Yamaguchi University, Yoshida 1677-1, Yamaguchi 753-8515, Japan

[d] Kazusa DNA Research Institute, 2-6-7 Kazusa-kamatari, Kisarazu Chiba, 292-0818 Japan

[e] Science Research Center, Organization for Research Initiatives, Yamaguchi University, Yoshida 1677-1, Yamaguchi 753-8515, Japan

[f] The United Graduate School of Agricultural Science, Tottori University, Tottori 680-8553 Japan

***Corresponding author:** Jun'ichi Mano

E-mail: mano@yamaguchi-u.ac.jp

Present address: The Institute of Advanced Energy, Kyoto University, Gokasho, Uji, 611-0011 Japan

†**Present address:** Graduate School of Agriculture, Kobe University, Rokkodai-cho 1-1, Kobe, 657-8501 Japan

ABSTRACT

Reactive carbonyl species (RCS), such as acrolein (Acr), are generated via the degradation of lipid peroxides and function both as signaling molecules and as cytotoxins downstream of reactive oxygen species (ROS). The aim of this study was to identify RCS-scavenging compounds, acting as secondary antioxidants, in plants. We established an HPLC-based method to sensitively evaluate the RCS-scavenging ability of compounds, using Acr as a representative RCS. Among 80% ethanol extracts of 46 angiosperm species, the highest scavenging activities were observed in garlic, spinach, avocado, broccoli, and lotus, representing a diverse range of plant families. The active ingredient from garlic cloves was identified as *S*-allyl cysteine sulfoxide (alliin), an amino acid typical of *Allium* species, which trapped up to two Acr molecules at its amino group. Notably, *S*-(1*E*)-propenyl cysteine sulfoxide (isoalliin), a structural analog of alliin and a major constituent of onion, showed even stronger Acr-scavenging activity. Isoalliin outperformed known Acr scavengers such as carnosine, epigallocatechin gallate, resveratrol, and hesperetin. These findings highlight isoalliin as a representative plant-derived RCS scavenger and emphasize the importance of *S*-alk(en)yl cysteine sulfoxides as potent Acr-scavenging compounds in plants. This study further suggests that structurally diverse RCS scavengers remain to be discovered among specialized metabolites in the plant kingdom.

KEYWORDS: *acrolein*, *alliin*, *isoalliin*, *methiin*, *reactive carbonyl species*

54 Plant life is exposed to potential threats from reactive oxygen species (ROS). During
55 photosynthesis in plants, singlet oxygen ($^1O_2$) and superoxide radical (O_2^-) are constantly
56 produced in chloroplasts (Asada 2006). Furthermore, the H_2O_2 generation flux in
57 peroxisomes in illuminated leaves of C3 plants reaches 25% of the flux of CO_2 fixation on
58 electron base. This is approximately 50 times greater than the ROS generation flux associated
59 with mitochondrial respiration (Foyer and Noctor, 2003). When plants suffer environmental
60 stress, i.e. any changes in the surrounding environmental conditions that are not favorable for
61 a plant, ROS production in the cells are increased due to the disturbance of metabolism (for
62 example, the rate of CO_2 fixation in leaves decreases at low temperatures or under drought).
63 ROS oxidize biomolecules such as proteins, nucleic acids and lipids, thereby impairing their
64 functions and damaging cells. As a defense system against ROS, plant cells are richly
65 equipped with multiple types of ROS-scavenging enzymes and antioxidants, thereby keeping
66 ROS concentrations low enough.
67 ROS exert their biological functions also via the secondary products 'reactive carbonyl
68 species (RCS)'. RCS is a collective name of the α,β-unsaturated aldehydes and ketones such
69 as acrolein (Acr) and 4-hydroxy-(*E*)-2-nonenal (HNE) that are formed via the degradation of
70 lipid peroxides (Esterbauer et al. 1991, Aldini et al. 2005, Mano 2012). An RCS molecule
71 readily forms an adduct with a protein at the thiol-, amino-, or imidazole group via Michael
72 addition of its β-carbon (Esterbauer et al. 1991), and cause alterations of the protein function

73 (Wible and Sutter 2017). In plants, more than a dozen types of RCS occur (Schauenstein et
74 al. 1977, Mano 2012) and their levels are increased under oxidative stress conditions (Yin et
75 al. 2010, Yamauchi et al. 2012, Biswas and Mano 2015, Roach et al. 2018, Sultana et al.
76 2022, 2024). Rises of RCS levels have significant physiological impacts. For example, the
77 genetic enhancement of the RCS-scavenging enzyme 2-alkenal reductase (AER) (Mano et al.
78 2002, 2005) in transgenic plants suppressed the increases in RCS levels due to salt stress
79 (Sultana et al. 2024), aluminium stress (Yin et al. 2010) and light stress (Mano et al. 2010)
80 and thereby conferred stress tolerance. Vice versa, the genetic deficiency of aldehyde
81 alkenal/one reductase (Yamauchi et al. 2012) and aldehyde oxidase (Srivastava et al. 2017,
82 Nurbekova et al. 2021) made the plants more susceptible to oxidative stress or senescence.
83 The plant defense system against RCS toxicity consists of several types of enzymes and small
84 molecules, as the system against ROS. As for enzymatic defense, several classes of enzymes
85 with distinct RCS-detoxifying reactions have been characterized such as AER (Mano et al.
86 2002, 2005), glutathione transferase tau isozymes (Mano et al. 2017, 2019a,b) and aldehyde-
87 scavenging enzymes such as aldo-keto reductase (Yamauchi et al. 2011), aldehyde
88 dehydrogenase (Sunker et al. 2003) and aldehyde oxidase (Srivastava et al. 2017, Nurbekova
89 et al. 2021).
90 RCS-scavenging small molecules also occur in plants. Thiol compounds such as cysteine
91 (Cys) and the reduced form of glutathione are excellent RCS scavengers (Esterbauer et al.

92 1975). Various polyphenols also have the RCS scavenging ability. Zhu et al. (2009)
93 compared the RCS scavenging ability of a dozen tea polyphenols *in vitro* and found that nine
94 of them, including epigallocatechin gallate (EGCG), showed a high Acr-scavenging activity.
95 The reaction of EGCG and Acr starts with a nucleophilic attack of the carbon at position 8 on
96 the EGCG A-ring on the *β*-carbon of Acr, thus forming a Michael adduct. Subsequent aldol
97 condensation produces a ring structure (Huang, et al., 2020). One EGCG molecule can bind
98 up to three Acr molecules (Sugimoto, et al., 2021). Acr-scavenging reactions have been also
99 characterized for other polyphenols and their glycosides such as resveratrol, hesperetin
100 (Wang, et al., 2015), ferulic acid (Tao, et al., 2019), pelargonidin (Colzani, et al., 2018),
101 myricetin (Zhang, et al., 2020) and cyanidin-3-*O*-glucoside (Song, et al., 2021).
102 Amino compounds also have RCS-scavenging potential. The primary amino group in γ-
103 aminobutyric acid (GABA), L-Ala and L-Ser serves as a Michael acceptor to bind up to two
104 molecules of Acr (Jiang et al. 2020a, Zou et al. 2021). Recently it was reported that *S*-allyl
105 cysteine sulfoxide (alliin), an amino acid typical of *Allium* species, can scavenge Acr at a
106 high speed although the reaction mechanism has yet to be clarified (Uemura et al. 2023).
107 Theophylline, a purine derivative found in tea, forms a Michael adduct between its secondary
108 amine and the *β*-carbon of Acr at a high rate (Jiang, et al., 2020b). Interestingly, animals
109 contain RCS-scavenging dipeptides carnosine, homocarnosine, and anserine (Aldini et al.
110 2002) in brain and muscle. The amino and imidazole groups of these histidine-containing

111 dipeptides react as Michael acceptors (Aldini et al., 2005), allowing them to be excellent RCS
112 scavengers (Aldini et al., 2002; Liu et al., 2003; Carini et al., 2003). Exogenous application
113 of these dipeptides to plant cells or seedlings suppressed the RCS levels and mitigated
114 oxidative injury, without affecting ROS levels (Biswas and Mano, 2015; Sultana et al., 2022),
115 showing that RCS-scavenging compounds can protect plants as the "secondary antioxidants".
116 In this study, we aimed at discovering RCS-scavenging compounds in plants. Employing Acr
117 as a representative RCS, we evaluated RCS-scavenging ability of dozens of angiosperms.
118 Garlic cloves showed the highest content of Acr-scavenging ability, which was attributed to
119 alliin, a garlic-typical amino acid. We found that isoalliin and methiin, the cysteine
120 derivatives relative to alliin, also showed excellent Acr-scavenging ability and revealed the
121 reaction mechanism. Potential of plant specialized compounds as the secondary antioxidants
122 is discussed.
123

124 **Materials and Methods**

125 ***Chemicals*** Alliin and methiin were purchased from LKT Laboratories (Saint Paul, MN).
126 Carnosine, fluorescein, and HNE dimethyl acetal (HNE-DMA) were purchased from Sigma-
127 Aldrich Japan (Tokyo), and isoalliin from Nagara Science Co. (Gifu, Japan). Anserine nitrate
128 was purchased from Fujifilm Wako Pure Chemical (Osaka, Japan). 2,4-
129 Dinitrophenylhydrazine (DNPH), purchased from Fujifilm Wako, was purified by

130 recrystallization in acetonitrile and kept in acetonitrile until use (Mano et al. 2022). All other
131 chemicals were of analytical grade. Acr was prepared on the day of use by hydrolysis of the
132 acetal, as follows. Acrolein dimethyl acetal (Tokyo Chemical Industry, Tokyo, Japan) was
133 dissolved in 100 mM HCl aqueous solution at 40˚C for 40 min. The solution was then
134 neutralized with $NaHCO_3$ and further incubated at 25˚C for 2 h. The concentration of Acr was
135 determined from the absorbance at 215 nm with an extinction coefficient of 15.0 mM^{-1} cm^{-1}
136 (in water).

137 ***Plant Materials*** Bamboo (*Phyllostachys heterocycla*) shoots and yuzu (*Citrus junos*) fruits
138 were harvested from Yamaguchi University's experimental field. Following materials of fresh
139 plants were purchased from grocery stores in Yamaguchi (Japan) between April and December
140 2018: Apple (*Malus domestica*) fruits, asparagus (*Asparagus officinalis*) shoots, avocado
141 (*Persea americana*) fruits, bell pepper (*Capsicum annuum* 'Grossum') fruits, bitter melon
142 (*Momordica charantia* var. *pavel*) fruits, broccoli (*Brassica oleracea* var. italica) buds, carrot
143 (*Daucus carota* subsp. *sativus*) roots, cherry (*Cerasus avium*) fruits, chestnuts (*Castanea*
144 *crenata*), Chinese yam (*Dioscorea polystachya*) roots, common ginger (*Zingiber officinale*)
145 rhizomes, edible burdock (*Arctium lappa*) roots, eggplant (*Solanum melongena*) fruits, fig
146 (*Ficus carica*) fruits, garlic (*Allium sativum*) cloves, grape (*Vitis labruscana* 'Pione') fruits,
147 green onion (*Allium fistulosum*) leaves, guava (*Psidium guajava*) fruits, Haskap berry
148 (*Lonicera caerulea* var. *emphyllocalyx*) fruits, Indian gooseberry (*Phyllanthus emblica*) fruits,

149 Japanese apricot (*Prunus mume*) fruits, Japanese butterbur (*Petasites japonicus*) stalks,
150 Japanese ginger (*Zingiber mioga*) shoots, Jun-sai (*Bransenia shreberi*) leaves, Kaki persimmon
151 (*Diospyros kaki*) fruits, kiwifruit (*Actinidia deliciosa*) fruits, Korean lettuce (*Lactuca sativa*)
152 leaves, loquat (*Rhaphiolepis bibas*) fruits, lotus (*Nelumbo nucifera*) rhizomes, Mandarin
153 orange (*Citrus unshiu*) fruits, mulkhiya (*Corchorus olitorius*) leaves, okra (*Abelmoschus*
154 *esculentus*) fruits, onion (*Allium cepa*) bulbs, parsley (*Petroselinum crispum*) leaves, pea
155 (*Pisum sativum*) seeds, perilla (*Perilla frutescens* var. *crispa*) leaves, pitaya (*Hylocereus*
156 *undatus*) fruits, plum (*Prunus salicina*) fruits, spinach (*Spinacia oleacea*) leaves, star fruit
157 (*Averrhoa carambola*) fruits, strawberry (*Fragaria* × *ananassa*) achenes, taro (*Colocasia*
158 *esculentai*) tubers, watermelon (*Citrullus lanatus*) fruits, and white radish (*Raphanus*
159 *sativus* var. *hortensis*) roots.

160 ***Plant Extract Preparation*** An edible portion (10 g) taken from a fresh sample was
161 homogenized in 80% (v/v) ethanol (20 mL) using a kitchen blender and filtered through a layer
162 of Miracloth (Sigma-Aldrich Japan). The filtrate was acidified with HCl (10 mM final) to
163 facilitate protein precipitation. It was centrifuged after 10 minutes of incubation at 25˚C, and
164 the resulting supernatant was neutralized with sodium bicarbonate. The volume of
165 deproteinized extract was measured.

166 ***Determination of the Acr-scavenging ability*** A reaction mixture containing 200 μM Acr, 50
167 mM potassium phosphate pH 6.8, and a plant extract was incubated at 30˚C for 10 min. One

168 volume of the mixture was then added to 6.35 volumes of acetonitrile containing 4 mM DNPH

169 and 0.4 M formic acid and incubated at 30˚C for 60 min. The resulting hydrazone solution was

170 filtered through a 0.45 μm filter (Millex LH; Merck, Darmstadt, Germany) and analyzed by

171 HPLC, as follows. The hydrazone solution (10 μL) was injected into a Zorbax ODS column

172 (4.6 × 250 mm, 5 μm; Agilent Technologies Japan, Hachioji, Japan) kept at 40˚C and separated

173 in a 1.0 mL min^{-1} flow of 75% (v/v) acetonitrile in water (isocratic elution) with a high-pressure

174 pump (2690 Separation Module, Waters Corp., Milford, MA). The hydrazone was detected

175 with a UV-visible detector (2487 Absorbance Detector, Waters) at 370 nm.

176 The decrease rate (v) of Acr concentration in the reaction mixture (in mol Acr consumed s^{-1} L^{-}

177 ^{1}) was used to calculate the Acr-scavenging ability of the plant extract per unit volume (in mol

178 Acr s^{-1} (L extract)$^{-1}$) by multiplying v by the volume ratio P (reaction mixture/plant extract) as

179 follows:

180 Acr-scavenging ability per unit volume of plant extract (mol s^{-1} (L extract)$^{-1}$)

181 = v (mol Acr scavenged L^{-1} s^{-1}) × P

182 The Acr-scavenging ability content in the original sample, as mol Acr consumed s^{-1} (g

183 sample)$^{-1}$, was then calculated from the extraction efficiency E (L extract (g sample)$^{-1}$) as

184 follows:

185 Acr-scavenging ability content (mol s^{-1} (g sample)$^{-1}$)

186 = Acr-scavenging ability of the extract (mol s^{-1} L^{-1}) × 1 (L) × E (L extract (g sample)$^{-1}$)

187 ***Purification of the Acr-scavenging component from garlic cloves*** Garlic cloves (40 g) were
188 homogenized in 80% (v/v) ethanol (80 mL) using a kitchen blender, filtered through two layers
189 of Miracloth, and centrifuged to remove insoluble debris. The supernatant was freeze-dried to
190 obtain 7.6 g of material, which was dissolved in distilled water (15 mL) and loaded onto a
191 preparative hydrophilic column (Universal Column Premium Amino 30 μm, 3.0 × 16.5 cm;
192 Yamazen Corp., Osaka, Japan) with a medium pressure chromatography system (EPCLC AI-
193 580; Yamazen Corp.) equipped with a detector (fixed wavelength at 254 nm). Chromatography
194 was performed at a flow rate of 20 mL/min under the following solvent conditions: solvent A:
195 acetonitrile:10 mM ammonium acetate in water (88:12, v/v); solvent B: acetonitrile:100 mM
196 ammonium acetate in water (1:1, v/v). The gradient program consisted of 0–16 min isocratic
197 elution of 0% B, 16–56 min of a linear gradient from 0% to 100% B, and 56–80 min isocratic
198 elution of 100% B. The fraction size was 20 mL. Each fraction was freeze-dried and then
199 dissolved in 2 mL of distilled water, and its Acr-scavenging ability was determined as
200 described above. The most active fraction was then separated on a Unison UK-Amino Column
201 (3 μm, 4.6×100 mm; Imtakt, Kyoto, Japan) with an HPLC apparatus equipped with an LH-40
202 liquid handler and an SPD-10AVP UV-VIS detector (Shimadzu Corp., Kyoto, Japan).
203 Chromatography was performed at a flow rate of 0.6 mL min^{-1} with the following multistep
204 gradient elution: 0–10 min isocratic elution of 0% B; 10–35 min of a linear gradient from 0%
205 to 100% B; 35–50 min isocratic elution of 100% B; 50–55 min of a linear gradient from 100%

206 to 0% B; and, finally, 55–90 min isocratic elution of 0% B. The fraction size was 1.8 mL. The
207 elution profile was monitored at 220 nm for nonspecific detection of organic substances. After
208 40 separation runs (50 μL injection per run), identical fractions were accumulated, freeze-dried,
209 and dissolved in a smaller volume to determine the Acr-scavenging ability.

210 ***LC-MS/MS analysis*** Chromatographic separation was performed on a hydrophilic Intrada
211 Amino Acid column (3 μm, 3 × 100 mm; Imtakt) with a Vanquish UHPLC System (Thermo
212 Fisher Scientific, Waltham, MA). A 5-μL aliquot of the sample was injected into the column
213 and eluted at a flow rate of 0.4 mL min^{-1} under the following solvent conditions: solvent A:
214 0.3% (v/v) in acetonitrile; solvent B: 0.1 M ammonium formate in water:acetonitrile (80:20,
215 v/v). The gradient program was as follows: 0–10 min isocratic elution of 15% B; 10–25 min
216 of a linear gradient from 15% to 60% B; 25–40 min isocratic elution of 60% B; 40–45 min of
217 a linear gradient from 60% to 15% B; and finally 45–50 min isocratic elution of 15% B. The
218 column temperature was set to 40˚C. Mass spectra were acquired using an Orbitrap Exploris
219 120 mass spectrometer (Thermo Fisher Scientific) equipped with an H-ESI source, with
220 acquisition in positive ion mode. The source parameters were as follows: capillary voltage of
221 3.5 kV in positive ion mode, ion transfer tube temperature of 325˚C, vaporizer temperature of
222 350˚C, sheath gas flow of 50 units, auxiliary gas flow of 10 units, and sweep gas of 1 unit. A
223 full scan was performed in the mass-to-charge ratio (*m*/*z*) range of 100–1000, with a resolution

224 of 120,000 at *m*/*z* 200. Tandem MS information was acquired in tMS^2 mode with a resolution

225 of 12,000 and HCD collision energies of 15, 30, and 45.

226

227 **Results and Discussion**

228 ***Comparison of Acr-scavenging ability of plants***

229 For choosing a starting material suitable for purifying RCS-scavenging compounds, we first

230 collected various plant samples broadly in the angiosperm phylogeny. To obtain samples in

231 such a variety in short time, we obtained them (46 species in total), mainly fruits and vegetables,

232 from local retail stores (see Materials and Methods). We extracted plants with 80% ethanol

233 because we targeted polar compounds rather than polyphenols, which have been extensively

234 investigated (Colzani, et al., 2018; Huang, et al., 2020; Sugimoto, et al., 2021; Tao, et al.,

235 2019; Wang, et al., 2015; Zhang, et al., 2020; Zhu, et al., 2009). This extract was deproteinized

236 by acid treatment, then neutralized, and its Acr-scavenging rate was determined. To survey

237 RCS scavengers that can react rapidly with Acr, we determined Acr consumption in the initial

238 10 minutes in our assay. The initial Acr concentration was set at 200 μM, mimicking

239 physiological concentration, which was estimated on the following observation. A typical Acr

240 content in salt-stressed *A. thaliana* seedlings is 200 nmol (g fresh weight)$^{-1}$ (Sultana, et al.,

241 2022). From this value, Acr concentration of 200 μM in the tissue was calculated on a simple

242 assumption that the Acr molecules occur in the tissue in a homogenous solution of 1 mL

243 volume per gram tissue weight. The reaction temperature was set at 30˚C to simulate field
244 conditions.

245 Fig. 1 summarizes the Acr-scavenging ability on the fresh weight base of the plant materials.
246 Most plant materials showed significant levels of Acr-scavenging ability, thus indicating that
247 many plants contain Acr-scavenging compounds. The highest Acr-scavenging ability content
248 (in nmol Acr scavenged s^{-1} (g fresh weight)$^{-1}$) were 1.39 for garlic cloves, 0.99 for spinach
249 leaves, 0.96 for avocado fruits, 0.92 for lotus rhizomes, 0.91 for broccoli buds, 0.82 for
250 chestnuts, 0.70 for bamboo shoots, 0.67 for onion bulbs, and 0.65 for both Chinese yam roots
251 and white radish roots. These plants, when placed in the angiosperm phylogeny tree (Cole, et
252 al., 2019), were distributed to different orders of taxa (Fig. 1). We chose garlic cloves as the
253 starting material for purification to identify an Acr-scavenging compound.

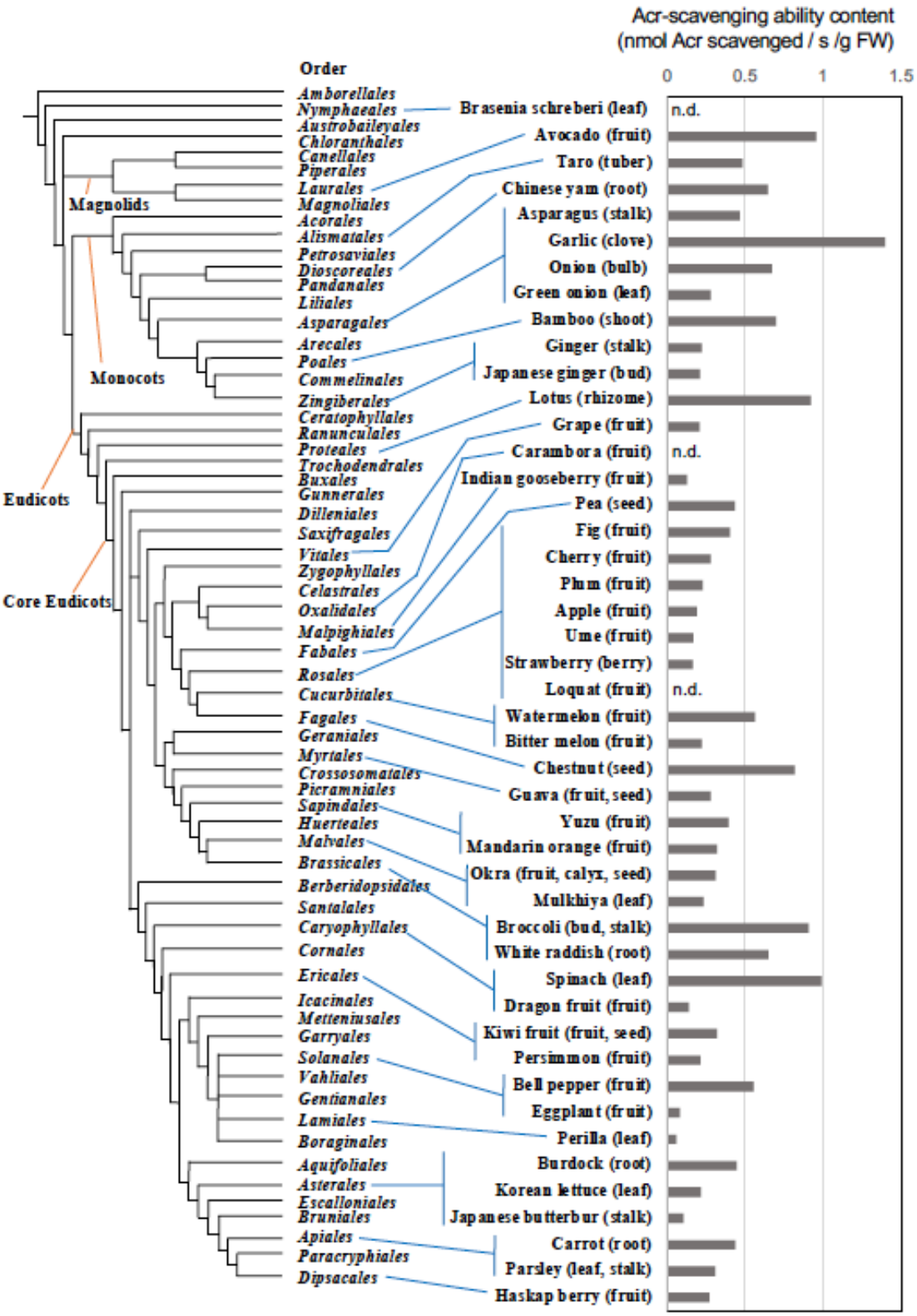

Figure 1. Acr-scavenging ability contents of plant materials. Plant extracts (80% ethanol) were deproteinized, neutralized, and tested for the Acr-scavenging ability as in Materials and Methods. Average of two runs. The phylogenic tree was constructed using the Angiosperm Phylogeny Poster (Cole et al. 2019) as a guide.

254

255

256 ***Purification of Acr-scavenging components from garlic extract***

257 Garlic clove extract was first separated by preparative amino column chromatography
258 (Supplementary Fig. S1A), which showed a single prominent peak of Acr-scavenging ability
259 in fractions #13, #14, and #15. We scaled up the sample amount and the column size, as
260 described in the Materials and Methods section, collected the active fractions, concentrated and
261 purified them using an analytical HPLC column. The resulting fraction #8 had a high Acr-
262 scavenging ability (Supplemental Fig. S1B). We then analyzed this fraction by LC-MS/MS.
263 Total ion chromatography (*m*/*z* 100–1000) revealed two major components: a broad peak
264 eluted at 15.3–16.6 min with *m*/*z* 178.0528 and a narrow peak at 18.87 min with *m*/*z* 258.1096
265 (Fig. 2A, black trace).

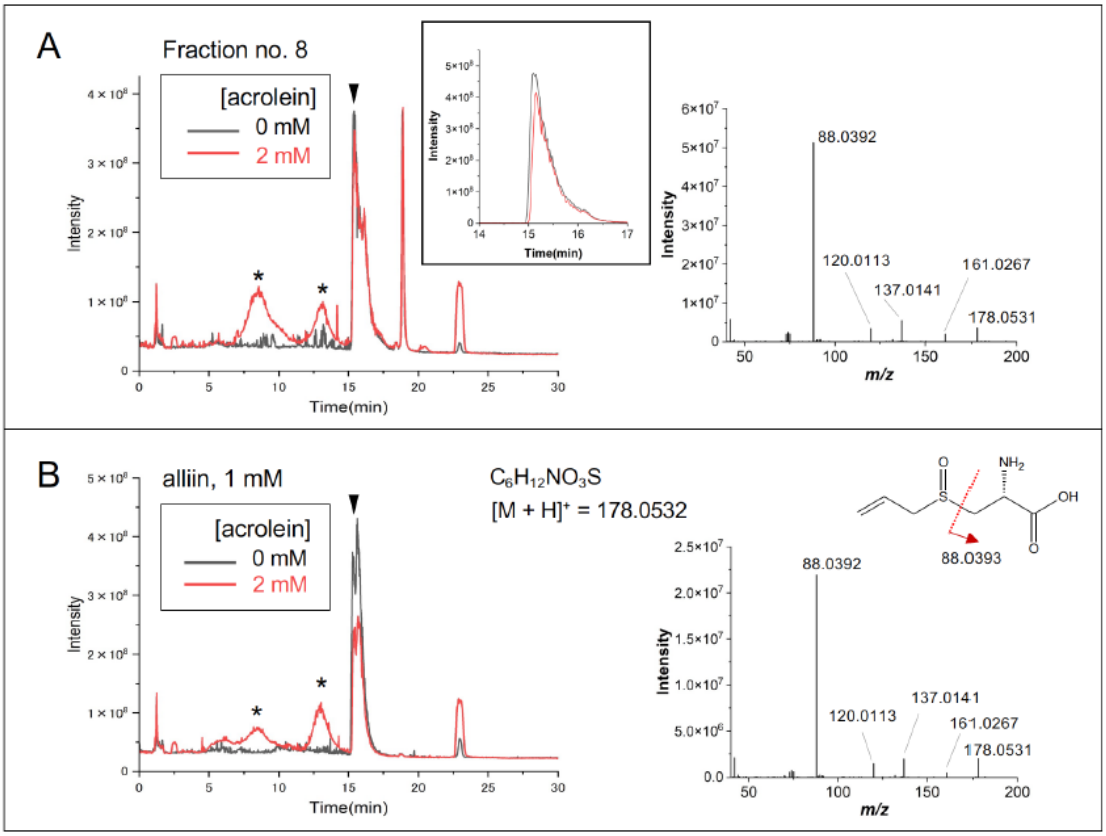

Figure 2. LC-MS/MS evidence that alliin is the acrolein-scavenging substance in the fraction no. 8 from the Unizon UK-Amino Column.

To clarify which component is the Acr scavenger, we mixed fraction #8 with Acr and examined the changes in the total ion chromatogram. The addition of Acr at 2 mM resulted in a significant decrease in the 15.3–16.6 min peak (Fig. 2A, inset), while that of the 18.87 min peak was unchanged, thus suggesting that the *m/z* 178.0528 signal represented the Acr scavenger in fraction #8. Addition of Acr to fraction #8 generated two new broad peaks at 8.57 (*m/z* 290.1056) and 13.16 min (*m/z* 234.0795) (Fig. 2A, asterisks). The *m/z* values of these peaks matched hypothetical Acr adducts to the *m/z* 178.0528 compound; the 13.16 min peak corresponded to a mono-Acr adduct (mass increment 56.0265, matching the molecular weight

274 of Acr (C_3H_4O)), and the 8.57 min peak a di-Acr adduct (mass increment 112.0526)., these

275 were due to the reaction products between the *m/z* 178.0528 compound and acrolein; the 13.16

276 min peak corresponding to

277 Assuming that the *m/z* 178.0528 ion represents a $[M + H]^+$ ion, the elemental composition

278 of the molecule was deduced as $C_6H_{11}NO_3S$. Retrieval of the corresponding compounds in

279 the databases AraCyc (Mueller, et al., 2003), PlantCyc (Plant Metabolic Network (PMN):

280 https://pmn.plantcyc.org/organism-summary?object=PLANT, on www.plantcyc.org, Jan 15,

281 2022), and KEGG (Kanehisa, et al., 2000) using the software package Compound Discoverer

282 3.0 (Thermo Fisher Scientific), resulted in *S*-allyl-cysteine sulfoxide (alliin; $C_6H_{11}NO_3S$,

283 177.22 g mol^{-1}) as the most probable candidate.

284 Alliin is an amino acid sulfoxide characteristic of garlic, accounting for about 30% (w/w) of

285 total free amino acids in garlic cloves (Ueda, et al., 1991), and is a precursor of allicin, the

286 major compound of garlic odor (Stoll and Seebeck, 1948). In the LC-MS/MS analysis,

287 authentic L-alliin eluted as a broad peak ranging from 15.2–16.7 min with an *m/z* of 178.0532

288 (Fig. 2B). The MS^2 spectrum of this parent ion (*m/z* 178.0532) matched the spectrum of the

289 *m/z* 178.0528 ion of the Acr scavenger in fraction #8 (Fig. 2A). The addition of Acr to alliin

290 decreased the alliin peak and generated two broad peaks at 8.20 (*m/z* 290.1056) and 13.02 min

291 (*m/z* 234.0795) (Fig. 2B), as observed for fraction #8. Thus, the Acr-scavenging component in

292 the purified fraction was identified as alliin.

293 ***Reaction mechanism of alliin with Acr*** Uemura et al. (2023) has reported that alliin has a high

294 capacity to scavenge Acr. Its reaction mechanism with Acr, yet to be elucidated, could be

295 similar to that of an amino compound; i.e. the Michael addition of the β-carbon to the amino

296 nitrogen, and the second addition of Acr to the same nitrogen, followed by the intramolecular

297 aldol condensation to form a nitrogen-containing heterocycle (Carini et al. 2003). When alliin

298 was incubated with Acr, larger MS signals of the mono-Acr adduct (*m/z* 234.0795, eluted at

299 8.20 min) and the di-Acr adduct (*m/z* 290.1056, 13.02 min) were observed as increasing

300 concentration of Acr (Fig. 3A, B). In addition, another signal at *m/z* 272.0950 arose in higher

301 Acr concentration (Fig. 3C). On the assumption that it represented a $[M + H]^+$ ion, the atomic

302 composition of the compound was deduced as $C_{12}H_{17}NO_4S$. We presumed that this signal

303 corresponded to a dehydrated product of the di-Acr adduct.

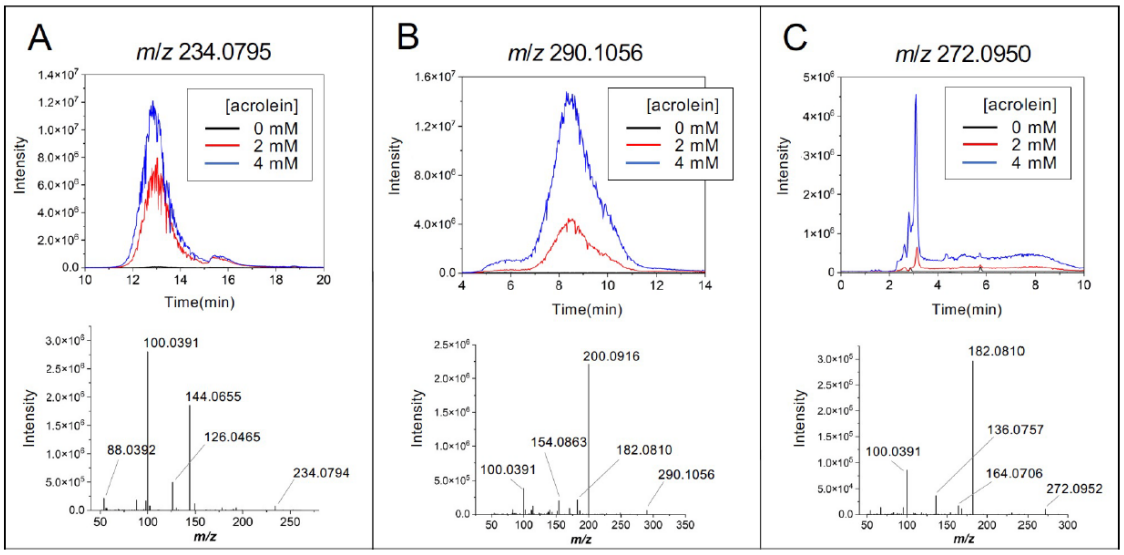

Figure 3. LC-MS/MS results of alliin-acrolein adducts.

304

305 We have purified this putative dehydrated product of the di-Acr adduct and determined its
306 structure with NMR. The deduced structure corresponded to the N^b-(3-formyl-3,4-
307 dehydropiperidino) derivative of alliin (Table 1), indicating that the amino group of alliin
308 accepted two molecules of Acr, as expected. Specifically, one Acr molecule adds to the amino
309 group (Michael-type reaction), then the resulting secondary amino group undergoes Michael
310 addition with another Acr molecule to form the $(Acr)_2$ adduct, which then undergoes aldol
311 condensation to form a nitrogen-containing heterocycle (Figure 4). The MS^2 spectra for the
312 Acr adducts support this mechanism; the spectrum for the mono-Acr adduct contained a
313 product ion at *m/z* 144.0655, the deduced atomic composition for which ($C_6H_{10}NO_3$) matched
314 the fragment generated by cleavage between the sulfur atom and the *β*-carbon of the amino
315 acid, the same cleavage position as in alliin (Fig. 2B). Similarly, the MS^2 spectra of the di-Acr

Table 1. ^{1}H NMR (400 MHz) and ^{13}C NMR (500 MHz) chemical shift data of the purified adduct of *m/z* 272.0950. Deduced structure of the dehydrated product of $(Acr)_2$-alliin adduct and a possible LC-MS/MS fragment ion structure are shown.

NMR data			Structural formula of the dehydrated product of $(Acr)_2$-alliin adduct	Fragment ion (+) of LC-MS/MS
No.	δ_H	δ_C		
1	5.52	124.85		
2	5.94	125.03		
3	3.60, 3.80	54.2		
4	3.27, 3.33	49.97		
5	3.7	63.68		
6	-	174.82		
7	2.87, 3.06	45.9	**exact mass 271.08728**	***m/z* 182.0810**
8	2.61	26.81		
9	7.18	152.41		
10	-	138.06		
11	9.35	195.6		
12	3.5	45.48		

316 adduct and its dehydrated product contained product ions at *m*/*z* 200.0917 (Fig. 3B) and *m*/*z*

317 182.0811 (Fig. 3C), which correspond to the fragments at the same cleavage position of the

318 deduced compounds, respectively.

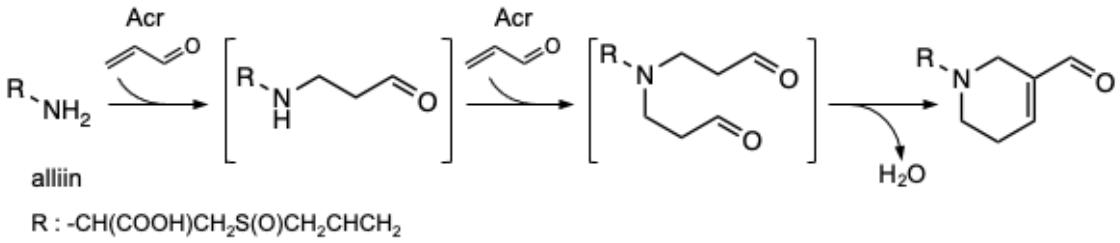

Figure 4. Possible reactions of alliin (R-NH_2) with Acr.

319

320

321 ***Comparison of the Acr-scavenging ability of S-alk(en)yl cysteine sulfoxides, amino***

322 ***compounds, and polyphenols***

323 Plants in the *Allium* family are rich in alliin-analogous *S*-alk(en)yl cysteine sulfoxides, such as

324 *S*-propenylcysteine sulfoxide (isoalliin) in onion (*A. cepa*) and *S*-methylcysteine sulfoxide

325 (methiin) in Oriental garlic (*A. tuberosum*) (Yamazaki, et al., 2011). Isoalliin and methiin also

326 formed mono-Acr and $(Acr)_2$ adducts and the dehydration product of the $(Acr)_2$ adduct, as did

327 alliin (Supplementary Fig. S3 and S4). The Acr-scavenging rates of these *S*-alk(en)yl cysteine

328 sulfoxides were 120–150 μM Acr in 30 min, when the reaction was started with 1 mM Acr and

329 1 mM scavenger (Table 2A). These rates were comparable to, or even higher than, those for

330 carnosine and anserine, Acr-scavenging dipeptides in animals (Carini, et al., 2003; Spaas, et

331 al., 2021).

332 As compared with broader variety of amino compounds, these *S*-alk(en)yl cysteine sulfoxides
333 excelled GABA and most of protein-constituting amino acids such as Met, His, Lys, Arg and
334 Gly for the Acr-scavenging rate. Such high Acr-scavenging rate for *S*-alk(en)yl cysteine
335 sulfoxides appears to be attributed to the presence of sulfoxide close to the amino carbon.
336 Indeed, methionine sulfoxide, in which the sulfoxide is one carbon further away, showed a
337 significantly faster Acr-scavenging rate than other amino acids lacking a sulfoxide although its
338 rate was slower than *S*-alk(en)yl cysteine sulfoxides (Table 2A).
339 We also compared the *S*-alk(en)yl cysteine sulfoxides with polyphenols that can scavenge
340 Acr. Isoalliin, methiin and alliin outperformed EGCG in scavenging Acr (Table 2A). To test
341 hydrophobic polyphenols resveratrol and hesperetin (Wang, et al., 2015), a separate experiment
342 was performed in 10% DMSO solution (Table 2B). Reaction time was set to 5 h because these
343 polyphenols scavenged Acr slowly in our preliminary experiments. Under these conditions,
344 alliin scavenged Acr faster than EGCG, resveratrol, and hesperetin. Theophylline, another type
345 of Acr scavenger (Jiang, et al., 2020b) showed an Acr-scavenging rate comparable to that for
346 hesperetin and much slower than that for EGCG and alliin (Table 2B).
347

348 **Table 2** (A) Comparison of Acr-scavenging rate of amino compounds. Acr (1 mM) was
349 incubated with a scavenger (1 mM) in 50 mM potassium phosphate, pH 7.0, at 30˚C for 30
350 min. The remaining Acr was determined by HPLC after derivatization with DNPH, as
351 described in the Materials and Methods section. Acr consumption (concentration in the
352 reaction mixture) in 30 min is shown. (B) Comparison of Acr-scavenging rate for alliin,
353 polyphenols, and theophylline. Acr (1 mM) was incubated with a scavenger (1 mM) in 10%
354 DMSO, 50 mM potassium phosphate, pH 7.0, at 30˚C for 5 h. Acr consumption in 5 h is
355 shown. The values shown are the average and standard error of three independent runs.
356 Different letters in the Statistics column represent significantly different values ($P < 0.05$,
357 Tukey's test).

A	Compound	Acr consumption (μM in 30 min)	Statistics
	Isoalliin	153.8 ± 6.5	a
	Methiin	144.5 ± 14.0	ab
	Alliin	126.8 ± 5.4	bc
	Carnosine	114.3 ± 1.3	cd
	Anserine	99.4 ± 5.5	de
	Methionine sulfoxide	86.0 ± 8.3	e
	Histidine	63.9 ± 6.0	f
	Lysine	59.5 ± 8.9	f
	Phenylalanine	57.5 ± 0.9	f
	EGCG	45.4 ± 5.2	f
	Arginine	44.7 ± 6.3	f
	Histamine	40.1 ± 8.4	fg
	Methionine	22.7 ± 8.7	gh
	GABA	10.6 ± 5.9	h
	β-Alanine	6.5 ± 3.7	h

358

B	Compound	Acr consumption (μM in 5 h)	Statistics
	Alliin	419.1 ± 3.0	a
	EGCG	282.0 ± 4.6	b
	Resveratrol	31.8 ± 1.5	c
	Hesperetin	18.9 ± 1.0	d
	Theophylline	17.9 ± 3.6	d

359

360 ***RCS scavenging compounds are present in many plant species*** Because RCS are secondary
361 toxic products derived from ROS, plants have evolved multiple enzymatic and non-enzymatic
362 mechanisms to mitigate their harmful effects (Mano et al. 2019a,b). In this study, we
363 established a method to evaluate the RCS-scavenging ability of plant extracts and demonstrated
364 that *S*-alk(en)yl cysteine sulfoxides, amino acids characteristic of *Allium* family, are highly
365 efficient Acr scavengers. Among them, isoalliin, the major sulfoxide in onion, exhibited the
366 strongest Acr-scavenging activity, surpassing not only its structural analog alliin but also other
367 well-known plant-derived and animal-derived scavengers. This finding identifies isoalliin as a
368 representative plant RCS scavenger and underscores the contribution of *Allium* metabolites to
369 the chemical defense system against carbonyl stress.

370 It is noteworthy that the presence of a sulfoxide group in close proximity to the amino
371 carbon markedly enhances the Michael acceptor reactivity of the amino group, thereby
372 conferring the high RCS-scavenging capacity observed in S-alk(en)yl cysteine sulfoxides.
373 Consequently, the RCS-scavenging property of a compound appears to be governed by the
374 cooperative action of two or more functional groups, rather than by the reactivity of a single
375 moiety alone. More broadly, our findings suggest that structurally diverse, and as yet
376 unexplored, plant metabolites may play critical roles in mitigating oxidative damage through
377 RCS detoxification.

ABBREVIATIONS

Acr, acrolein; DNP-, dinitrophenylhydrazo-; DNPH, 2,4-dinitrophenylhydrazine; FW, fresh weight; GSH, the reduced form of glutathione; HNE, 4-hydroxy-(*E*)-2-nonenal; LOOH, lipid peroxide; RCS, reactive carbonyl species; ROS, reactive oxygen species.

AUTHOR CONTRIBUTION

Conceptualization: J. M. and D.S.; Investigation: A.H., N.T.; Methodology: J.M., C.N., A.H., N.T., Y.M., K.M.; Roles/Writing - original draft: A.H., N.T., Writing - review & editing; A.H., J.M., Funding acquisition: J.M., D.S.; Supervision: J.M.

ACKNOWLEDGMENT

The authors would like to express their gratitude to Ryoma Oishi and Suzuka Monden for their technical assistance and to Prof. Toshihiro Murafuji, Yamaguchi University, for discussion.

FUNDING

This work was supported by the Ministry of Agriculture, Forestry and Fisheries of Japan, by KAKENHI Grants (nos. 17K19909 and 20H03278) from the Japan Society for the Promotion

397 of Science (to J. M.), and by Yamaguchi University Project for Formation of the Core Research
398 Project. This work resulted from the use of research equipment shared in the MEXT Project
399 for promoting public utilization of advanced research infrastructure (Program for supporting
400 the construction of core facilities) Grant Number JPMXS0440400022.

401

402 **FIGURE CAPTIONS**

403 **Fig 1.** Acr-scavenging ability contents of plant materials. Plant extracts (80% ethanol) were
404 deproteinized, neutralized, and tested for the Acr-scavenging ability as in Materials and
405 Methods. Average of two runs. The phylogenic tree was constructed using the Angiosperm
406 Phylogeny Poster (Cole et al. 2019) as a guide.

407 **Fig. 2.** LC-MS/MS evidence that alliin is the Acr-scavenging substance in fraction #8 using a
408 Unizon UK-Amino Column. A: Total ion chromatograms (*m*/*z* range 100–1000) of fraction
409 #8 with 2 mM Acr (red trace) and without it (black). The MS/MS spectrum of the *m*/*z*
410 178.0528 signal at 15.4 min is shown on the right. Inset: expanded chromatogram of the 15.1
411 min peak. B: Total ion chromatograms (*m*/*z* range 100–1000) of 1 mM alliin with 2 mM Acr
412 (red trace) and without it (black). The MS/MS spectrum of the *m*/*z* 178.0532 signal at 15.4
413 min (arrowhead) is shown on the right. Asterisks show possible Acr reaction products with
414 the scavenging compound (A) or with alliin (B).

415 **Fig. 3.** LC-MS/MS results for alliin-Acr adducts. An authentic alliin preparation (5 mM) was
416 mixed with various concentrations of Acr, incubated for 1 h, and subjected to LC-MS/MS
417 analysis. A: Extracted ion chromatograms of the mono-Acr adduct of alliin (*m*/*z* 234.0795). B:
418 Extracted ion chromatograms of the $(Acr)_2$ adduct (*m*/*z* 290.1056). C: Extracted ion
419 chromatograms of the dehydrated products from the di-Acr adduct (*m*/*z* 272.0950). The
420 corresponding parent ion MS/MS spectrum is shown at the bottom of panels A–C.

421 **Fig. 4.** Possible reactions of alliin with Acr.

422

423 **ASSOCIATED CONTENTS**

424 Supporting information is available.

425 Two chromatographic results for the purification of Acr-scavenging substances from garlic
426 extract (Fig. S1), MS spectrum of the 15.42 min peak of fraction #8 (Fig. S2), LC-MS/MS
427 results for the reaction products of isoalliin and Acr (Fig. S3), and LC-MS/MS results for the
428 reaction products of methiin and Acr (Fig. S4).

429

430

431 **REFERENCES**

432 G. Aldini, M. Carini, G. Beretta, S. Bradamante, R. M. Facino, Carnosine is a quencher of 4-
433 hydroxy-nonenal: through what mechanism of reaction? Biochem. Biophys. Res.
434 Commun. 298 (2002) 699-706, https://doi.org/10.1016/S0006-291X(02)02545-7.

435 G. Aldini, I. Facino, G. Beretta, M. Carini, Carnosine and related dipeptides as quenchers of
436 reactive carbonyl speices: From structural studies to therapeutic perspecitves,
437 BioFactors 24 (2005) 77-87, https://dx.doi.org/10.1002/biof.5520240109.

438 G. Aldini, I. Dalle-Donne, R. M. Facino, A. Milzani, M. Carini, Intervention strategies to
439 inhibit protein carbonylation by lipoxidation-derived reactive carbonyls, Med. Res. Rev.
440 27 (2007) 817-868, https://doi.org/10.1002/med.20073.

441 G. Aldini, M. Orioli, R. Rossoni, F. Savi, P. Braidotti, G. Vistoli, K.-J. Yeum, G. Negrisoli, M.
442 Carini, The carbonyl scavenger carnosine ameliorates dyslipidaemia and renal function
443 in Zucker obese rats. J. Cell. Mol. Med. 15 (2011) 1339-1354,
444 https://doi.org/10.1111/j.1582-4934.2010.01101.x.

445 K. Asada, Production and scavenging of reactive oxygen species in chloroplasts and their
446 functions, Plant Physiol. 141 (2006) 391-396, https://doi.org/10.1104/pp.106.082040.

447 M. S. Biswas, J. Mano, Lipid peroxide-derived short-chain carbonyls mediate hydrogen
448 peroxide-induced and salt-induced programmed cell death in plants, Plant Physiol.
449 168 (2015) 885–898, https://doi.org/10.1104/pp.115.256834.
450 M. Carini, G. Aldini, G. Beretta, E. Arlandini, R. M. Facino, Acrolein-sequestering ability of
451 endogenous dipeptides: characterization of carnosine and homocarnosine/acrolein
452 adducts by electrospray ionization tandem mass spectrometry, J. Mass Spectr. 38
453 (2003) 996-1006, https://doi.org/10.1002/jms.517.

454 T. C. Cole, H. H. Hilger, P. Stevens, Angiosperm Phylogeny Poster (APP) – Flowering plant
455 systematics, PeerJ Preprints 7 (2019) e2320v6,
456 https://doi.org/10.7287/peerj.preprints.2320v6

457 M. Colzani, L. Regazzoni, A. Criscuolo, G. Baron, M. Carini, G. Vistoli, Y.-M. Lee, S. I. Han,
458 G. Aldini, K.-J. Yeum, Isotopic labelling for the characterisation of HNE-sequestering
459 agents in plant-based extracts and its application for the identification of anthocyanidins
460 in black rice with giant embryo, Free Rad. Res. 52 (2018) 896-906,
461 https://doi.org/10.1080/10715762.2018.1490735.

462 H. Esterbauer, H. Zollner, N. Scholtz, Reaction of glutathione with conjugated carbonyls, Z.
463 Naturforsch. 30c (1975) 466-473, http://doi.org/10.1515/znc-1975-7-808.

464 H. Esterbauer, R. J. Schaur H. Zollner, Chemistry and biochemistry of 4-hydroxynonenal,
465 malonaldehyde and related aldehydes, Free Rad. Biol. Med. 11 (1991) 81-128,
466 https://doi.org/10.1016/0891-5849(91)90192-6.

467 C. H. Foyer, G. Noctor, Redox sensing and signalling associated with reactive oxygen in
468 chloroplasts, peroxisomes and mitochondria, Physiol. Plant. 119 (2003) 355-364,
469 https://doi.org/10.1034/j.1399-3054.2003.00223.x.

470 Q. Huang, Y. Zhu, L. Lv, S. Sang, Translating in vitro acrolein-trapping capacities of tea
471 polyphenol and soy genistein to in vivo situations is mediated by the bioavailability and
472 biotransformation of individual polyphenols, Mol. Nutr. Food Res. 64 (2020) 1900274,
473 https://doi.org/10.1002/mnfr.201900274.

474 K. Jiang, Z. Yin, P. Zhou, H. Guo, C. Huang, G. Zhang, W. Hu, S. Ou, J. Ou, The scavenging
475 capacity of γ-aminobutyric acid for acrolein and the cytooxicity of the formed adduct,
476 Food Funct. 11 (2020a) 7736, https://doi.org/10.1039/C9FO02518A.

477 X. Jiang, D. Zhang, Y. Lu, L. Lv, Acrolein-trapping mechanism of theophylline in green tea,
478 coffee, and cocoa: Speedy and successful, J. Agric. Food Chem. 68 (2020b) 9718-9724,
479 https://doi.org/10.1021/acs.jafc.0c03895.

480 M. Kanehisa, S. Goto, KEGG: Kyoto Encyclopedia of Genes and Genomes, Nucleic Acids Res.
481 28 (2000) 27-30, https://doi.org/10.1093/nar/28.1.27.

482 M. Knieper, A. Veihhause, K.-J. Dietz, Oxylipins and reactive carbonyls as regulators of the
483 plant redox and reactive oxygen species network under stress. Antioxidants 12 (2023)
484 814, https://doi.org/10.3390/antiox12040814.

485 Y. Liu, G. Xu, L. M. Sayre, Carnosine 1nhibits (*E*)-4-hydroxy-2-nonenal-induced protein
486 cross-linking: structural characterization of carnosine−HNE adducts, Chem. Res.
487 Toxicol. 16 (2003) 1589-1597, https://doi.org/10.1021/tx034160a.

488 J. Mano, Reactive carbonyl species: their production from lipid peroxides, action in
489 environmental stress, and the detoxification mechanism, Plant Physiol. Biochem. 59
490 (2012) 90-97, https://doi.org/10.1016/j.plaphy.2012.03.010.

491 J. Mano, Y. Torii, S. Hayashi, K. Takimoto, K. Matsui, K. Nakamura, D. Inzé, E.
492 Babiychuk, S. Kushnir, K. Asada, The NADPH:quinone oxidoreductase P1-ζ-
493 crystallin in Arabidopsis catalyzes the α,β-hydrogenation of 2-alkenals: detoxication
494 of the lipid peroxide-derived reactive aldehydes, Plant Cell Physiol. 43 (2002) 1445-
495 1455, https://doi.org/10.1093/pcp/pcf187.

496 J. Mano, E. Belles-Boix, E. Babiychuk, D. Inzé, E. Hiraoka, K. Takimoto, L. Slooten, K.
497 Asada, S. Kushnir, Protection against photooxidative injury of tobacco leaves by 2-
498 alkenal reductase. Detoxication of lipid peroxide-derived reactive carbonyls, Plant
499 Physiol. 139 (2005) 1773–1783, https://doi.org/10.1104/pp.105.070391.

500 J. Mano, K. Tokushige, H. Mizoguchi, H. Fujii, S. Khorobrykh, Accumulation of lipid
501 peroxide-derived, toxic α,β-unsaturated aldehydes (E)-2-pentenal, acrolein and (E)-2-
502 hexenal in leaves under photoinhibitory illumination. Plant Biotechnol. 27 (2010)
503 193–197, https://doi.org/10.5511/plantbiotechnology.27.193.
504 J. Mano, A. Ishibashi, H. Muneuchi, C. Morita, H. Sakai, M. S. Biswas, T. Koeduka, S.
505 Kitajima, Acrolein-detoxifying isozymes of glutathione transferase in plants, Planta
506 245 (2017) 255-264, https://doi.org/10.1007/s00425-016-2604-5.
507 J. Mano, S. Kanameda, R. Kuramitsu, N. Matsuura, Y. Yamauchi, Detoxification of reactive
508 carbonyl species by glutathione transferase Tau isozymes, Front. Plant Sci. 10 (2019a)
509 487, https://doi.org/10.3389/fpls.2019.00487.
510 J. Mano, M. S. Biswas, K. Sugimoto, Reactive carbonyl species: A missing link in ROS
511 signaling, Plants 8 (2019b) 391, https://doi.org/10.3390/plants8100391.

512 L. A. Mueller, P. Zhang, S. Y. Rhee, AraCyc: A biochemical pathway database for Arabidopsis.
513 Plant Physiol.,132 (2003) 453-460, https://doi.org/10.1104/pp.102.017236.

514 Z. Nurbekova, S. Srivastava, D. Standing, A. Kurmanbayeva, A. Bekturova, A. Soltabayeva,
515 D. Oshanova, V. Turečková, M. Strnad, M. S. Biswas, J. Mano, M. Sagi, Arabidopsis
516 aldehyde oxidase 3, known to oxidize abscisic aldehyde to ABA, protects leaves from
517 aldehyde toxicity, Plant J. 108 (2021) 1439-1455, https://doi.org/10.1111/tpj.15521.

518 T. Roach, W. Stöggl, T. Baur, I. Kranner, Distress and eustress of reactive electrophiles and
519 relevance to light stress, Free Rad. Biol. Med., 122 (2018) 65-73,
520 https://doi.org/10.1016/j.freeradbiomed.2018.03.030.

521 E. Schauenstein, H. sterbauer, H. Zollner, Aldehyde in Biological Systems: Their Natural
522 Occurrence and Biological Activities; Pion, 1977, pp. 589–590.

523 X. Song, Y. Lu, Y. Lu, L. Lv, Adduct formation of acrolein with cyanidin-*O*-glucoside and its
524 degradants/metabolites during thermal processing or in vivo after consumption of red
525 bayberry, J. Agric. Food Chem. 69 (2021) 13143-13154,
526 https://doi.org/10.1021/acs.jafc.1c05727.

527 J. Spaas, W. M. A. Franssen, C. Keytsman, L. Blancquaert, T. Vanmierlo, J. Bogie, B. Broux,
528 N. Hellings, J. van Horssen, D. K. Posa, D. Hoetker, S. P. Baba, W. Derave, B. O.
529 Eijnde, Carnosine quenches the reactive carbonyl acrolein in the central nervous system
530 and attenuates autoimmune neuroinflammation, J. Neuroinflam., 18 (2021) 255,
531 https://doi.org/10.1186/s12974-021-02306-9.

532 S. Srivastava, C. Brychkova, D. Yarmolinsky, A. Soltabayeva, T. Samani, M. Sagi, Aldehyde
533 oxidase 4 plays a critical role in delaying silique senescence by catalyzing aldehyde
534 detoxification, Plant Physiol. 173 (2017) 1977–1997,
535 https://doi.org/10.1104/pp.16.01939.

A. Stoll, E. Seebeck, Über Alliin, die genuine Muttersubstanz des Knoblauchöls. 1. Mitteilung über Allium-Substanzen, Helv. Chim. Acta 31 (1948) 189-210, https://doi.org/10.1002/hlca.19480310140.

K. Sugimoto, Y. Matsuoka, K. Sakai, N. Fujiya, H. Fujii, J. Mano, Catechins in green tea powder (matcha) are heat-stable scavengers of acrolein, a lipid peroxide-derived reactive carbonyl species, Food Chem. 355 (2021) 129403, https://doi.org/10.1016/j.foodchem.2021.129403.

M. S. Sultana, S. Yamamoto, M. S. Biswas, C. Sakurai, H. Isoai, J. Mano, Histidine-containing dipeptides mitigate salt stress in plants by scavenging reactive carbonyl species, J. Agric. Food Chem. 70 (2022) 11169-11178, https://doi.org/10.1021/acs.jafc.2c03800.

M. S. Sultana, C. Sakurai, M. S. Biswas, L. Szabados, J. Mano, Accumulation of reactive carbonyl species in roots as the primary cause of salt stress-induced growth retardation of *Arabidopsis thaliana,* Physiol. Plant. 176 (2024) e14198, https://doi.org/10.1111/ppl.14198.

R. Sunker, D. Bartels, H.-H. Kirch, Overexpression of a stress-inducible aldehyde dehydrogenase gene from *Arabidopsis thaliana* in transgenic plants improves stress tolerance, Plant J. 35 (2003) 452–464, https://doi.org/10.1046/j.1365-313X.2003.01819.x.

554 Z.-h. Tao, C. Li, X.-f. Zu, Y.-j. Pan, Scavenging activity and mechanism study of ferulic acid
555 against reactive carbonyl species acrolein, J. Zhejiang Univ.-Science B 20 (2019) 868-
556 876, https://doi.org/10.1631/jzus.B1900211.

557 Y. Ueda, H. Kawajiri, N. Miyamura, R. Miyajima, Content of some sulfur-containing
558 components and free amino acids in various strains of garlic, Nippon Shokuhin Kogyo
559 Gakkaishi 38 (1991) 429-434, https://doi.org/10.3136/nskkk1962.38.429.

560 T. Uemura, M. Uchida, M. Nakamura, M. Shimekake, A. Sakamoto, Y. Terui, K. Higashi, I.
561 Ishii, K. Kashiwagi, K. Igarashi, A search for acrolein scavengers among food
562 components, Amino Acids 55 (2023) 509-518, https://doi.org/10.1007/s00726-023-
563 03248-7.

564 W. Wang, Y. Qi, J. R. Rocca, P. J. Sarnoski, A. Jia, L. Gu, Scavenging of toxic Acrolein by
565 resveratrol and hesperetin and identification of adducts, J. Agric. Food Chem. 63 (2015)
566 9488-9495, https://doi.org/10.1021/acs.jafc.5b03949.

567 R. S. Wible, T. R. Sutter, Soft cysteine signaling network: the functional significance of
568 cysteine in protein function and the soft acids/bases thiol chemistry that facilitates
569 cysteine modification, Chem. Res. Toxicol. 30 (2005) 729-762,
570 https://doi.org/10.1021/acs.chemrestox.6b00428.

571 Y. Yamauchi, A. Hasegawa, A. Taninaka, M. Mizutani, Y. Sugimoto, NADPH-dependent
572 reductases involved in the detoxification of reactive carbonyls in plants, J. Biol.
573 Chem. 286 (2011) 6999–7009, https://doi.org/10.1074/jbc.M110.202226.
574 Y. Yamauchi, A. Hasegawa, M. Mizutani, Y. Sugimoto, Chloroplastic NADPH-dependent
575 alkenal/one oxidoreductase contributes to the detoxification of reactive carbonyls
576 produced under oxidative stress, FEBS Lett. 586 (2012) 1208-1213,
577 https://doi.org/10.1016/j.febslet.2012.03.013.
578 Y. Yamazaki, K. Iwasaki, M. Mikami, A. Yogihashi, Distribution of eleven flavor precursors,
579 *S*-alk(en)yl-L-cysteine derivatives in seven Allium vegetables, Food Sci. Technol.
580 Res. 17 (2011) 55-62, https://doi.org/10.3136/fstr.17.55.
581 L. Yin, J. Mano, S. Wang, W. Tsuji, K. Tanaka, The involvement of lipid peroxide-derived
582 aldehydes in aluminum toxicity of tobacco roots, Plant Physiol. 152 (2010) 1406–1417,
583 https://doi.org/10.1104/pp.109.151449.
584 D. Zhang, Z. Jiang, L. Xiao, Y. Lu, S. Sang, L. Lv, Mechanistic studies of inhibition on
585 acrolein by myricetin, Food Chem. 323 (2020) 126788,
586 https://doi.org/10.1016/j.foodchem.2020.126788.
587 Q. Zhu, Z.-P. Zheng, K. W. Cheng, J. J. Wu, S. Zhang, Y. S. Tang, K. H. Sze, J. Chen, F. Chen,
588 M. Wang, Natural polyphenols as direct trapping agents of lipid peroxidation-derived

589 acrolein and 4-hydroxy-trans-2-nonenal, Chem. Res. Toxicol. 22 (2009) 1721-1727,
590 https://doi.org/10.1021/tx900221s.

591 Z. Zou, Z. Yin, J. Ou, J. Zheng, F. Liu, C. Huang, S. Ou, Identification of adducts formed
592 between acrolein and alanine or serine in fried potato crips and the cytotoxicity-
593 lowering effect of acrolein in three cell lines, Food Chem. 361 (2021) 130164,
594 https://doi.org/10.1016/j.foodchem.2021.130164.

595

596 **Declaration of generative AI and AI-assisted technologies in the writing process**

597 During the preparation of this work the authors used DeepL, ChatGPT and Google Gemini in
598 order to improve the English. After using this tool/service, the authors reviewed and edited the
599 content as needed and take full responsibility for the content of the publication.

600

601

602